A New Direct Deformation Sensor for Active Compensation of Positioning Errors in Large Milling Machines

Francesco Biral
University of Trento
via Mesiano 77, I-38050 Trento, Italy
Phone: +390461882451, fax: +390461882599
e-mail: francesco.biral@ing.unitn.it

Paolo Bosetti
University of Trento
via Mesiano 77, I-38050 Trento, Italy
Phone: +390461882451, fax: +390461882599
e-mail: paolo.bosetti@ing.unitn.it

Roberto Oboe
University of Trento
via Mesiano 77, I-38050 Trento, Italy
Phone: +390461882584, fax: +390461882599
e-mail: roberto.oboe@ing.unitn.it

Francesco Tondini
University of Trento
via Mesiano 77, I-38050 Trento, Italy
Phone: +390461882578, fax: +390461882599
e-mail: f.tondini@studenti.unitn.it

Abstract— **The positioning accuracy of large boring and milling machines (with axes travel larger than 5 m) is severely affected by structural deformations. Heat induced deformations, long-period deformation of foundations, and the machining process itself, cause time-dependent structural deformations of the machine body, which are difficult to model and to predict. In order to overcome these difficulties and to enhance the positioning accuracy, a composite sensor has been designed and tested, which allows direct and continuous (up to 250 Hz) measurement of geometrical deformations on machine structural elements. The present paper *i*) presents the operating principles of the proposed composite sensor, which is based on an array of Fiber-optics Bragg Gratings (FBG), *ii*) discusses requisites and performances of the sensor as well as the algorithm used to calculate the deformed shape as a function of the sensor output, *iii*) illustrates the results of a finite elements virtual model aimed to demonstrate the feasibility and to evaluate the expected performance of the sensor, and *iv*) validates the model by showing the results obtained by a sensor prototype giving a real-time measurement of the deformed shape of a structural beam.**

I. Introduction

There is a wide industrial interest in enhancing the positioning accuracy of CNC machine tools, and this particularly applies to the case of large milling and boring machines. In fact, geometrical errors and thermo-structural deformations are particularly harmful when the total travel of the linear axes is order of 5 m, since they usually result in an overall positioning accuracy, which is rarely smaller than 0.1 mm. The two main sources of errors may be described as [1]–[6]:

- geometrical errors, which can be expressed as the shape errors affecting the structural elements of the machine, and which may be considered as time-independent on a machining cycle time-scale;
- thermo-structural deformations, which are effects of thermal, structural, and dynamic loads acting on the machine structure, and which are intrinsically time-dependent.

Fig. 1. PAMA SpeedRam 2000 CNC Milling/boring machine (travels: headstock 5 m, column 4 m, ram 1.2 m, spindle 1 m).

The present paper focuses on measurement and compensation of the second, time-dependent error source, and illustrates a new composite sensor, named Direct Deformation Sensor (SDD), which allows the measurement of the deformed shape of main structural parts of a Cartesian, three axes, milling/boring machine, see for example Fig. 1. From a performance point-of-view, the originality of the proposed solution is the relatively high operative frequency of the sensor (about 100 Hz), which allows the measurement of the deformations on a time-scale compatible with the machining process.

II. SDD Working Principles

The sensor is realized with an array of instrumented beams, arranged as a two-dimensional reticular beam structure, with each beam having a strain sensor along the axial direction. When the reticular structure is bolted, node-by-node, on a structural component of a large milling machine (see Fig. 2), the longitudinal deformation of each sensor beam can be used to compute, by triangulation, the in-plane displacement of each node. Since the sensor nodes are rigidly fixed to the underlying structure, the deformed shape of the structure can be obtained, by interpolation, from the deformed position of the nodes (as shown in Fig. 5). For example, the three SDD sensors shown in Fig. 2 can be used to measure the deformed shape of the bed (waviness on xy plane, SDD1) and of the column (SDD2 for xy waviness and SDD3 for yz waviness).

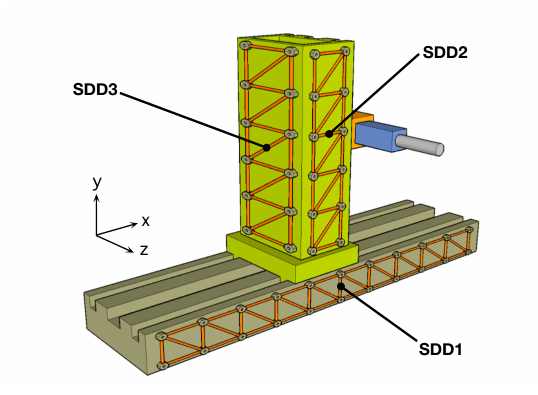

Fig. 2. Simplified model of a large milling machine (typical travels as for Fig. 1). Three reticular SDD sensors are shown on horizontal and on vertical elements.

The potential in error prediction and compensation of the simple concept above illustrated becomes even more interesting when the beams are equipped with Fiber-optic Bragg Gratings strain sensors (FBG, [7], [8]). In fact, beside to the resolution and accuracy levels suitable for the application, FBG sensors are particularly interesting since they have a nominal dynamic range from DC up to 250 Hz (using a wave-division-multiplexing interrogator, WDM [8]), which allows the detection and measurement of structural deformations acting on both very long time scale (like thermal deformations) and mildly short time scale (like deformations caused by dynamics and by structural loads). Additionally, and even more important for the present case, FBG sensors do not show any drift in measured strain value, allowing a direct comparison between instant and reference strain levels, even after long time periods and after repeated system shutdowns [8].

Taking as reference the numbering convention shown in Fig. 3, the planar coordinates of the ith node, $n_i = (x_i, y_i)$, can be related with the coordinates of the nodes n_{i-1} and n_{i-2} and with the length of the beams L_{2i-3} and L_{2i-4}:

$$\begin{cases} (x_i - x_{i-1})^2 + (y_i - y_{i-1})^2 &= L_{2i-3}^2 \\ (x_i - x_{i-2})^2 + (y_i - y_{i-2})^2 &= L_{2i-4}^2 \end{cases} \quad (1)$$

under the condition $x_i > x_{i-1}$.

These two simultaneous equations can be solved for (x_i, y_i), giving:

$$\begin{cases} x_i = f_x(x_{i-1}, y_{i-1}, x_{i-2}, y_{i-2}, L_{2i-3}, L_{2i-4}) \\ y_i = f_y(x_{i-1}, y_{i-1}, x_{i-2}, y_{i-2}, L_{2i-3}, L_{2i-4}) \\ \qquad i = 3 \dots m \end{cases} \quad (2)$$

with the starting conditions:

$$\begin{aligned} n_1 &= (x_1, y_1) = (0, 0) \\ n_2 &= (x_2, y_2) = (0, y_0 + L_1) = (0, L_1) \end{aligned}$$

and where the actual expressions of f_x and f_y are omitted for the sake of brevity.

Note that (2) gives the deformed shape of the structure except for a rigid body rotation. By knowing the position of two nodes, for example n_2 and n_m in Fig. 3, the actual position of the remaining $n_1, n_3, n_4, \dots, n_{m-1}$ nodes can be obtained by rotating the coordinates of all the nodes about the node n_2 by the angle $\widehat{n_m n_2 n'_m}$, where n_m and n'_m are the positions of the mth node as calculated with the (2) and as accepted as known, respectively. For example, supposing that the vertical position of the nodes n_2 and n_m will remain fixed and that $n_2 = (0, 0)$, the angle of rigid body rotation, θ, can be expressed as:

$$\theta = \tan^{-1}\left(\frac{y_m - y_2}{x_m - x_2}\right) = \tan^{-1}\left(\frac{y_m}{x_m}\right) \quad (3)$$

and the corresponding positions of the remaining $m - 2$ nodes can be expressed as:

$$n'_i = R_\theta n_i \tag{4}$$

where R_θ is the rotation matrix

$$R_\theta = \begin{pmatrix} \cos\theta & -\sin\theta \\ \sin\theta & \cos\theta \end{pmatrix}$$

and n'_i is the rotated position of the ith node.

At this point it is worth noting that the deformed position of a generic point on the upper or lower surface of the structure attached to the SDD can be approximated with a suitable interpolating function passing through the upper or lower SDD nodes, respectively.

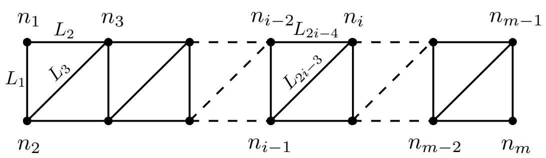

Fig. 3. Reference numbering for nodes and sensors.

III. Sensor FE Model

In order to investigate the feasibility of the composite sensor, a finite element model has been developed for a simplified machine headstock loaded with structural and thermal loads (see Fig. 4). Load intensities have been adjusted in order to have displacements comparable with those usually affecting large milling machines. The output signals of a "virtual" SDD with 12 mesh nodes (see Fig. 5) have been derived by interpolation of the displacement FEM solution at each SDD node location, rounded down to the actual FBG strain resolution (i. e. 10^{-6}).

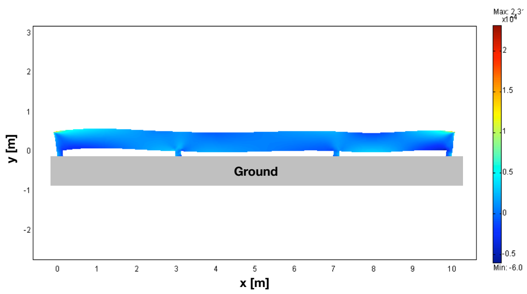

Fig. 4. Simplified FE model of the headstock structure of the reference machine under thermal and structural loads.

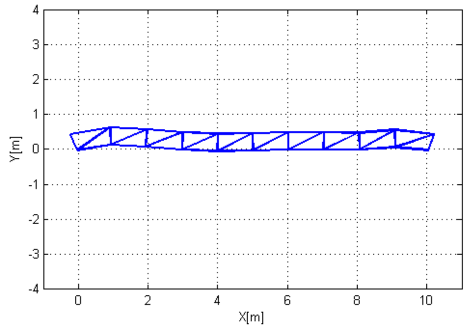

Fig. 5. Deformed shape of the reticular sensor (defomations magnification factor: 1000).

The y (vertical) displacement as resulting from the FEM model and as computed by the virtual SDD (using (2) and (4)) are reported in Fig. 6. The good agreement proves that the strain resolution of FBG sensors is sufficient in order to accurately measure deformations within the same order of magnitude of those usually affecting large milling machines. It is worth noting that, due to the reduced resolution of the virtual SDD, the difference between the two results reported in Fig. 6 is particularly small when displacements exceed about 50 μm, which is compatible with typical accuracy levels for large machine tools.

IV. SDD Prototype

On the basis of the positive results obtained from the FE model, a sensor prototype has been produced in order to investigate the effect of real design issues on SDD performance. For example, the model above described assumes that the SDD reticular structure is made of ideal hinge nodes (i.e. no transmitted moments) and beams with ideal linear elastic behavior, uniaxially loaded. In fact, only under these hypotheses one can hold the assumption that the length of the ith beam is linearly related with the strain measured by its respective strain sensor, ϵ_i, i.e.:

$$L_i = L_{i,0}\,(1 + \epsilon_i) \tag{5}$$

where $L_{i,0}$ is the reference length of the ith beam. The real SDD implementation, on the other hand, could be affected by non-ideal hinge behavior of the nodes as well as by contact non-linearities (e.g.: nut-thread-washer contacts), which could change (5) in:

$$L_i = L_{i,0}\,(1 + \epsilon_i) + \Delta L(\sigma_1) \tag{6}$$

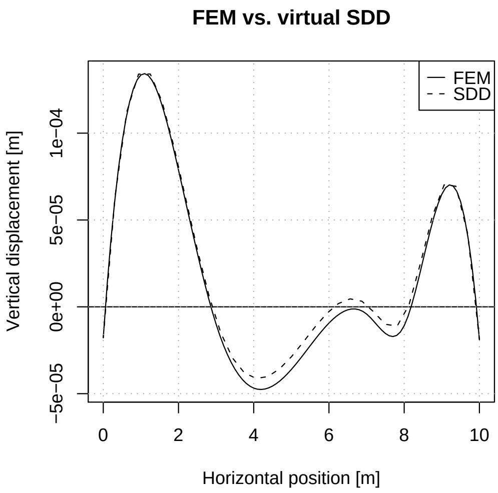

Fig. 6. Vertical displacement of the reference structure as a function of the horizontal position, as calculated by FE model and by the virtual SDD (strain resolution: $1{\times}10^{-6}$).

where ΔL is a function of the beam axial stress and depends on the actual mechanical behavior of beams and nodes .

A prototype SDD sensor is thus needed in order to ensure that the ΔL is small and not too heavily non-linear, so that it could be eventually approximated with a constant calibration factor, as in:

$$L_i = L_{i,0}\,(1 + k_i \epsilon_i) \tag{7}$$

where k_i is a calibration constant for the ith instrumented beam.

The concept model that has been proposed for the test bench is shown in Fig. 7. The bench is a reticular beam structure built with modular aluminium strut profiles having overall dimensions of 0.3 m × 0.3 m × 2.0 m. The actual SDD is constituted by a series of cylindrical rods attached to one lateral side of the bench structure by means of two series of solid beams fixed transversally to the bench structure (see the detail in Fig. 7). Each rod has an FBG sensor glued on its half-length, and the rod is pre-stressed by means of end nuts, so that no load inversion could affect the strain measurement.

This solution provides a modular test bench with a total weight of about 100 kg, which is easy to move and to load without the need for additional facilities.

The model has been effectively implemented as shown in Fig. 8, while the actual number of mesh elements has been reduced from 6 to 4 in order to reduce the cost. Two additional FBG sensors loosely mounted at both ends of the structure are used for temperature compensation [8]. The bench was then horizontally mounted on two end supports.

The array of FBG sensors constituting the SDD has been connected with a WDM interrogator (Micronoptics SI425, multiplexing frequency 250 Hz), which, in turn, was communicating the strain data to a personal computer via TCP/IP protocol. A special software tool has been developed allowing the real time computation and visualization of the deformed structure (see for example Fig. 9). Due to communication and computation issues, the actual maximum frequency for deformed shape computation has been reduced down to about 100 Hz.

Finally, the calibration constants for the instrumented beams, as defined in (7), have been calculated as

$$k_i = \frac{L_i - L_{i,0}}{L_{i,0}\,\epsilon_i} \tag{8}$$

where L_i and $L_{i,0}$ are the lengths of the ith beam, respectively, in unloaded and loaded condition — as measured with dial indicators — and ϵ_i is the strain signal of the ith FBG sensor. The resulting values of the calibration constants were almost the same for all the instrumented beams, with an average value of $k = 1.07 \pm 0.007$. This means that non ideal behavior of beams and nodes counts for about 7% of the beams deformation. Additionally, the relationship between applied load and strain values resulted to be linear within 1% over a range of 100–1000 N.

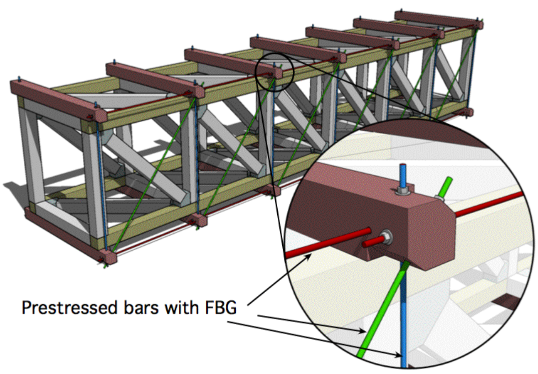

Fig. 7. Concept model for a test bench: a reticular beam with a superimposed grid of FBG sensors in horizontal, vertical, and 45°direction.

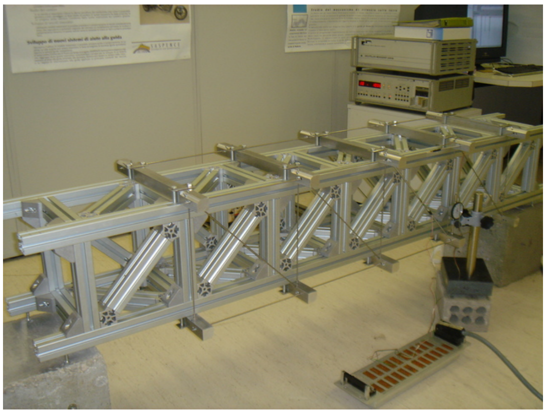

Fig. 8. Test bench with a four-meshes SDD prototype. A digital dial indicator used during the test is visible near the lower left corner of the picture.

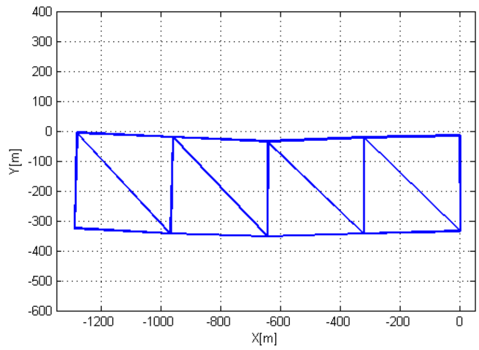

Fig. 9. Deformed shape for the test bench under vertical load applied at the middle span, as computed by the SDD (exaggerated).

V. Prototype Test Results

The four-meshes SDD shown in Fig. 8 has been tested accordingly to the following procedure:

1) reference strain level is zeroed for all the sensors in unloaded condition
2) one digital dial indicator (resolution 0.001 mm) is placed in contact with each SDD node along vertical direction, and zeroed in unloaded condition
3) a point load of 300 N is applied on the structure
4) the vertical displacement of each node as measured by dial indicators is recorded and compared with the corresponding quantity as computed by the SDD software (on the basis of (2), taking the two supporting points as fixed in order to calculate the rotation angle, (4)).

The test procedure has been replicated three times, applying the load on nodes 3, 5, and 7. The difference between the vertical position of nodes 4, 6, and 8 as measured by dial indicators and SDD resulted in an average value of 0.5 μm with a standard deviation of 0.9 μm. The Fig. 9 shows the deformed shape as computed by the SDD software, with node displacements magnified by a factor 1000.

The SDD prototype is thus suitable to describe the deformation of the attached structure within an accuracy of about 1 μm, which largely exceeds the typical accuracy of large CNC machine tools like that depicted in Fig. 1 (typically about 0.05 mm or more).

VI. Future developements

The sensor is still in a early development stage and needs further investigations especially on the following aspects:

- **Long-term static behavior**: as stated above, FBG strain sensors do not show any signal drift and do not require any re-calibration after shutdowns. Consequently, the SDD provides a measurement of the deformation of the attached structure with respect to a given reference state, which could eventually be the original as-installed machine state. Long-term accuracy and repeatability of SDD measurements are currently under investigation.
- **Dynamic behavior**: the relatively high frequency response of FBG sensors suggests the possibility to use the SDD output as a compensation signal even during machining operations. For example, deformations of the column caused by machining loads as well as inertia loads during maximum feed rate movements could eventually be compensated acting on headstock position. This aspect will be soon investigated by mounting the prototype shown in Fig. 7 as a vertical column onto the headstock of an horizontal linear axis. The numerical control will be programmed in order to compensate the horizontal headstock position with the horizontal deflection of a given reference point on the column, as computed by the SDD. The positioning error of the reference point on the column will then be measured by means of a laser doppler vibrometer, under different test conditions (e.g. im-

posed column deformation as resulting from internal loads, thermal gradients, or inertial loads).

- **Three-dimensional deformations**: though the SDD can accurately measure in-plane deformations of the attached structure, more complex deformations need three dimensional reticular sensor structures, probably as schematically shown on the column of the machine in Fig. 2. This is the most challenging application, and will probably be investigated on a real CNC machine tool like that shown in Fig. 1.
- **CNC integration**: different strategies for integration of SDD output with the CNC are possible and will be investigated. For example, depending on the actual dynamic performance of the SDD attached on a machine tool structural elements, the SDD signal will eventually require a suitable filtering in order to compensate mid-frequency deformation without causing instability to the CN control loop.

VII. Conclusions

The paper describes a prototype for a new composite sensor, called SDD, for active compensation of errors deriving from deformations of structural parts in large CNC machine tools. Although several different techniques and equipments have been proposed in order to measure and compensate the positioning error (see [5], [6]), the proposed sensor shows the following peculiar properties:

- the SDD can provide a real-time, instant measurement of the deformed shape of the attached structure, i.e., it can provide the deformed position of any given point of the structure by interpolation of the deformed position of SDD nodes;
- the strain sensors constituting the SDD are Fiber-optic Bragg Gratings (FBG), interrogated by a Wavelength-Division-Multiplexing spectrometer, which provide an absolute measurement of strain levels, do not suffer for drift even over very long time-scale observations, and easily compensate the temperature effect.

The paper illustrates the design of the prototype sensor and the results of static tests performed in order to estimate the sensor accuracy, which resulted being order of 1 μm in measuring the deflection of the attached beam structure over a span of 1.3 m.

Acknowledgment

The research presented in this work has been funded and contributed by PAMA S.p.A. (www.pama.it, Rovereto, TN, Italy).

References

[1] Y. Altintas, *Manufacturing automation*. Cambridge: Cambridge university press, 2000.

[2] E. P. Degarmo, J. T. Black, and R. A. Kohser, *Materials and Processes in Manufacturing*, 9th ed. John Wiley & Sons, 2003.

[3] E. H. Fung and S. M. Yang, “An approach to on-machine motion error measurement of a linear slide,” *Measurement*, vol. 29, no. 1, pp. 51–62, 2001.

[4] J. Choi, B. Min, and S. Lee, “Reduction of machining errors of a three-axis machine tool by on-machine measurement and error compensation system,” *Journal of Materials Processing Technology*, vol. 155-156, pp. 2056–2064, 2004.

[5] R. Ramesh, M. Mannan, and A. Poo, “Error compensation in machine tools — a review: Part I: geometric, cutting-force induced and fixture-dependent errors,” *International Journal of Machine Tools and Manufacture*, vol. 40, no. 9, pp. 1235–1256, July 2000.

[6] ——, “Error compensation in machine tools — a review: Part II: thermal errors,” *International Journal of Machine Tools Manufacture*, no. 40, pp. 1257–1284, 2000.

[7] P. Niewczas, A. Willshire, L. Dziuda, and J. McDonald, “Performance analysis of the fiber bragg grating interrogation system based on an arrayed waveguide grating,” *Instrumentation and Measurement, IEEE Transactions*, vol. 53, no. 4, pp. 1192 – 1196, Aug 2004.

[8] Y.-J. Rao, “In-fibre bragg grating sensors,” *Meas. Sci. Technol.*, vol. 8, pp. 355–375, 1997.